# Photosystem I Reduction in Diatoms: As Complex as the Green Lineage Systems but Less Efficient

Pilar Bernal-Bayard, Fernando P. Molina-Heredia, Manuel Hervás, and José A. Navarro*

Instituto de Bioquímica Vegetal y Fotosíntesis, Universidad de Sevilla & CSIC, Américo Vespucio 49, 41092 Sevilla, Spain

**S** *Supporting Information*

**ABSTRACT:** Diatoms occupy a key branch in the evolutionary tree of oxygen-evolving photosynthetic organisms. Here, the electron transfer reaction mechanism from cytochrome $c_6$ to photosystem I from the diatom *Phaeodactylum tricornutum* has been analyzed by laser-flash absorption spectroscopy. Kinetic traces of photosystem I reduction fit to biphasic curves, the analysis of the observed rate constants indicating that electron transfer occurs in a cytochrome $c_6$/photosystem I transient complex, which undergoes a reorganization process from the initial encounter complex to the optimized final configuration. The mild ionic strength dependence of the rate constants makes evident the relatively weak electrostatically attractive nature of the interaction. Taken together, these results indicate that the "red" *Phaeodactylum* system is less efficient than "green" systems, both in the formation of the properly arranged (cytochrome $c_6$/photosystem I) complex and in the electron transfer itself. The results obtained from cross-reactions with cytochrome $c_6$ and photosystem I from cyanobacteria, green algae, and plants shed light on the different evolutionary pathway of the electron transfer to photosystem I in diatoms with regard to the way that it evolved in higher plants.
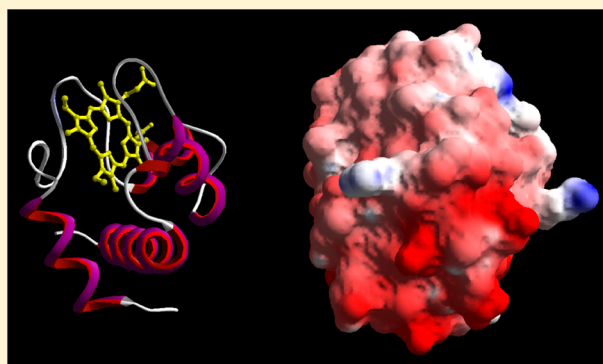
In photosynthetic organisms, electron transfer (ET) from cytochrome $b_6f$ to photosystem I (PSI) complexes, which are both membrane-embedded, is conducted by the two soluble metalloproteins cytochrome $c_6$ (Cyt) and plastocyanin (Pc).[1] PSI reduction has been extensively analyzed *in vitro* and *in vivo* in a wide variety of organisms, revealing that the kinetic mechanisms for the reaction of either Pc or Cyt with PSI from the same organism are similar, although they have increased in complexity and efficiency while evolving from prokaryotic cyanobacteria to green alga and plant eukaryotic organisms.[1–5]

In the green lineage of photosynthetic eukaryotes (green algae and higher plants), the donor proteins for PSI are very acidic and interact with a well-conserved positively charged docking site in PSI by means of strong attractive electrostatic interactions.[6–8] However, in cyanobacteria, both Pc and Cyt can be acidic, neutral, or basic, and thus, the role of electrostatic forces in the interaction with PSI varies accordingly.[1,9–11]

Diatoms belong to the red lineage of algae that diverged via evolution from the green lineage that evolved to higher plants.[12,13] Diatoms constitute the most abundant and diversified group of oceanic eukaryotic phytoplankton.[14,15] Approximately 40% of the 45−50 billion metric tons of organic matter yearly generated by oceanic photosynthesis can be traced back to diatoms.[16] In addition, because of their silicified walls, dead diatoms sinking fundamentally contribute to the sequestration of fixed carbon into the deep sea.[17] Thus, it is of great interest to determine the physiological behavior of diatoms and the facts that limit their growth and productivity.

In the last instance, the productivity of diatoms is related to their photosynthetic efficiency. In this sense, from both genetic analyses and biochemical studies, it is known that the photosynthetic ET chain in diatoms (as in other eukaryotic unicellular algae from the red lineage) possesses some peculiarities, arising from their double endosymbiotic origin. Thus, the composition of the extrinsic proteins at the lumenal side of photosystem II closely relates to cyanobacteria, as in diatoms this photosystem contains the three cyanobacterial-like extrinsic subunits PsbO, PsbU, and PsbV (or cytochrome $c_{550}$).[18] Also, the pigment composition of diatoms differs from that of other photosynthetic organisms as they have chlorophyll *c*/fucoxanthin-containing light-harvesting complexes (FCP) associated with the photosystems.[19,20] Moreover, while most cyanobacteria and unicellular green algae contain both the copper protein Pc and Cyt as alternative electron donors between the $b_6f$ and PSI complexes, the switch between both proteins being regulated by copper availability,[1] most diatoms are though to lack Pc, thus containing just Cyt as the only soluble carrier between these complexes,[21] with the noticeable exception of the oceanic centric diatom *Thalassiosira oceanica*, for which the constitutive (not regulated by copper) expression of an unusual Pc has been described.[22]

The coastal pennate diatom *Phaeodactylum tricornutum* (*Phaeodactylum* hereafter), in particular, has shown great flexibility in adapting to environmental changes, as it has been typically found in coastal areas with wide fluctuations in salinity, it can grow in the absence of silicon, and changes in cell shape can be stimulated by environmental conditions as it can exist in different morphotypes. The crystal structure and physicochemical features of Cyt from *Phaeodactylum* have been characterized, including the determination of its redox potential ($E'_m$ = 0.36 V at pH 7), which is similar to those of other Cyts.[21,23] Whereas the overall backbone structure of this cytochrome is similar to that of other prokaryotic or eukaryotic Cyts, the protein is very acidic (pI ≈ 4.5),[23] like other eukaryotic Cyts (pI ≈ 3.5−4.5). With respect to PSI, this complex has been purified from different diatoms, with a particular focus on the peculiar light-harvesting complexes of these organisms.[20,24−29] Among others, a PSI/FCP complex was isolated from the diatom *Phaeodactylum*,[20] and blue native polyacrylamide gel electrophoresis, gel filtration, and electron microscopy studies of this PSI/FCP sample revealed a monomeric complex comparable in size and shape to the PSI/LHCI complex of green algae.[20] Although a previous steady-state study has analyzed the Cyt oxidation rate by PSI purified samples of the centric diatom *Chaetoceros gracilis*,[26] no time-resolved studies of the ET process between diatom Cyt and PSI have been reported.

In this work, we have analyzed the interaction and the ET process between Cyt and PSI from *Phaeodactylum*. Moreover, taking into account the peculiar evolution of diatoms, we have studied the cross reactions between these two components of the photosynthetic chain with different prokaryotic and eukaryotic PSIs and Cyts, to obtain relevant data about the differences and similarities of the diatom couple with respect to other well-characterized systems and the evolution of the reaction mechanism in the different branches of photosynthetic organisms.

## ■ EXPERIMENTAL PROCEDURES

**Protein Purification.** Cyt from *Nostoc* sp. PCC 7119, *Synechocystis* sp. PCC 6803, and *Monoraphidium braunii* was purified as described previously.[30] Purification of Cyt from *Phaeodactylum* was conducted as a modification of the protocol described for *Monoraphidium* Cyt,[30] as follows. *Phaeodactylum* cells from photobioreactor outdoor cultures were obtained as a frozen paste from Easy Algae (Cádiz, Spain). Frozen cells were resuspended in 10 mM MES (pH 6.5), 2 mM KCl, 5 mM EDTA buffer, supplemented with protease inhibitors and DNase, and disrupted by two cycles in a French pressure cell at 20000 psi. Unbroken cells were separated by centrifugation at 5000g for 5 min, and the supernatant was centrifuged at 170000g for 20 min to remove most of the membrane fraction. After differential precipitation with streptomycin sulfate and ammonium sulfate[30] and extensive dialysis in 2 mM Tris-HCl (pH 8.0), the resulting Cyt sample was purified by fast performance liquid chromatography in one step by using a diethylaminoethyl-cellulose column (2 cm × 20 cm, gel volume of 60 mL, and elution flow of ∼20 mL/h) previously equilibrated with the same buffer. The Cyt was eluted by applying a 0.01 to 0.2 M NaCl linear gradient (total volume of 0.6 L). Pure protein fractions with an $A_{553}/A_{275}$ ratio close to 1.2 were pooled, suspended in 20 mM Tricine-KOH buffer (pH 7.5) after several cycles of concentration and dilution in an Amicon pressure filtration cell, concentrated, and finally frozen

at −80 °C until they were used. The concentration of the cytochrome was calculated using an extinction coefficient of 25.8 mM$^{-1}$ cm$^{-1}$ at 553 nm for the reduced form.[23]

*Nostoc* and *Arabidopsis thaliana* PSI were purified essentially as previously described.[2] PSI particles from *Phaeodactylum* were obtained by β-dodecyl maltoside (β-DM) solubilization taking as a starting point the protocol of Lepetit et al.[25] for the purification of FCP from the same organism, but with significant modifications. Frozen *Phaeodactylum* cells were resuspended in buffer A [10 mM MES (pH 6.5), 2 mM KCl, 5 mM EDTA, and 1 M sorbitol] and harvested by centrifugation (4000g for 10 min). All subsequent preparation steps were taken in dim light at 4 °C. The cells were resuspended in buffer B (buffer A without sorbitol) supplemented with protease inhibitors and DNase and disrupted by two cycles in a French pressure cell at 20000 psi. Unbroken cells were separated by centrifugation at 5000g for 5 min; the supernatant was centrifuged at 170000g for 30 min, and the pelleted thylakoids were resuspended in buffer B at a concentration of 1 mg of Chl/mL. At this point, the solution was frozen at −20 °C. With a 100 g wet weight of cells as a starting point, the yield of membranes was approximately 100−120 mg of chlorophyll. For the solubilization of thylakoid membranes, unfrozen suspensions were diluted to a concentration of 0.5 mg of Chl/mL with the same volume of 3% (w/v) β-DM, prepared in buffer B, to yield a final detergent:Chl ratio of 30:1 (w/w). The thylakoids were solubilized in the dark at 4 °C for 30 min while being continuously gently stirred. After solubilization, the solution was centrifuged at 170000g for 30 min to remove unsolubilized material. The resulting supernatant, containing the solubilized pigment/protein complexes, was loaded onto a continuous sucrose density gradient from 0.17 to 0.65 M sucrose, prepared in buffer B with 0.03% β-DM, and centrifuged at 135000g for 21 h. The lower mostly green band, including a small part of the upper brown material, was collected, extensively washed with buffer B with 0.03% β-DM, and concentrated on an Amicon pressure filtration cell fitted with a YM100 membrane, before being loaded onto a second sucrose density gradient, from 0.25 to 0.45 M, and centrifuged as described above. The lower green band, enriched in PSI, was collected, extensively washed with 20 mM Tricine-KOH (pH 7.5) with 0.03% β-DM, concentrated as described above, and stored at −80 °C until it was used. The P700 content of PSI samples was calculated from the photoinduced absorbance changes at 820 nm using the absorption coefficient of 6.5 mM$^{-1}$ cm$^{-1}$ determined by Mathis and Sétif.[31] The chlorophyll concentration was determined using the method of Arnon.[32] The chlorophyll:P700 ratio of the resulting PSI preparations was 185, with a final yield of ∼4 mg of chlorophyll.

**Laser-Flash Absorption Spectroscopy.** Kinetics of flash-induced absorbance changes associated with PSI photo-oxidation and further re-reduction by Cyt were followed at 830 nm as described by Hervás and Navarro,[33] except that the measuring detector was replaced with a SM1PD1A silicon photodiode (ThorLabs). Unless otherwise stated, the standard reaction mixture contained, in a final volume of 0.2 mL, 20 mM Tricine-KOH (pH 7.5), 10 mM MgCl₂, 0.03% β-DM, an amount of PSI particles equivalent to 0.35 or 0.5 mg of Chl/mL for the cyanobacterial or eukaryotic PSI, respectively, 0.1 mM methyl viologen, 2 mM sodium ascorbate, and Cyt at the indicated concentration. To study the effects of ionic strength, the concentration of either NaCl or MgCl₂ was progressively

increased in the reaction cell by adding small amounts of a concentrated stock solution. All the experiments were performed at 22 °C in a 1 mm path-length cuvette. Kinetic data collection and analyses were as previously described.[2,33] Typically, the estimated error in the observed rate constant was ≤15%. Values for the association ($k_{ON}$) and dissociation ($k_{OFF}$) rate constants for complex formation, the forward ($k_1$) and reverse ($k_{-1}$) rate constants for complex rearrangement, and the ET first-order rate constant ($k_{ET}$) were estimated according to the formalisms previously described[2,11,34] (see Figure S1 of the Supporting Information).

**Structural Models.** The structures of PsaF from *Phaeodactylum* CCAP1055/1 and *Nostoc* sp. PCC 7120 were modeled using Phyre[2] (http://www.sbg.bio.ic.ac.uk/phyre2/html/),[35] employing as templates the PsaF structures from pea [Protein Data Bank (PDB) entry 1jb0] and *Thermosynechococcus elongatus* (PDB entry 3lw5), respectively. The quality of the modeled structures was tested using PROCHECK.[36] Surface electrostatic potentials of Cyts and PsaF luminal loops were depicted using Swiss-Pdb Viewer[37] from either the three-dimensional available structures [cytochromes from *Monoraphidium*, *Phaeodactylum*, and *Thermosynechococcus* (PDB entries 1ctj, 3dmi, and 4eic, respectively)] and *Thermosynechococcus* and pea PsaF or the modeled ones (*Phaeodactylum* and *Nostoc* PsaF).

## ■ RESULTS

A yield of ~10 mg of Cyt was obtained from an 80 g wet weight of *Phaeodactylum* cells, by following a modification of previously described purification methods combining differential ammonium sulfate precipitation and ionic exchange chromatography.[30] It has been previously reported that the relative content of photosynthetic complexes in diatoms is lower than that in cyanobacteria or green alga cells.[20] Consequently, a large quantity of diatom cells (100 g) was required to achieve PSI purification (chlorophyll:$P_{700}$ ratio of ≈185), following detergent solubilization and two consecutive sucrose gradients, in the milligram quantities (on a chlorophyll basis) required for this study.

Upon analysis of the interaction of Cyt with PSI from *Phaeodactylum* by laser-flash absorption spectroscopy, kinetic traces corresponding to the re-reduction of photooxidized $P_{700}^+$ by Cyt have to be fit to biphasic curves (Figure 1), with a first, fast phase that becomes evident at heme protein concentrations as low as 20 $\mu$M (Figure 1; see also the top panel of Figure 2). The amplitude of this fast kinetic phase increases with an increasing Cyt concentration, reaching saturating values of 37% of the total laser-flash-induced absorbance change (Figure 2, top). The observed rate constant ($k_{obs}$) for such a fast phase is independent of donor protein concentration, with an average value of 23500 s$^{-1}$ ($t_{1/2}$ of ~30 $\mu$s) (Figure 2, top), thus indicating a first-order ET process occurring in a preformed [Cyt/PSI] transient complex, as previously described in other organisms.[1,2,38−40]

The Cyt concentration dependence of $k_{obs}$ for the second, slower phase of PSI reduction shows, however, a saturation profile (Figure 2, bottom). The theoretical $k_{obs}$ value [1030 s$^{-1}$ (not shown)], obtained by extrapolating to infinite donor protein concentration,[41] does not match the experimental $k_{obs}$ data for the fast phase, thus suggesting the occurrence of a limiting intermediate step between complex formation and ET, in good agreement with the reaction mechanism proposed for other donor/PSI systems:[1,2,10,38−40,42,43]
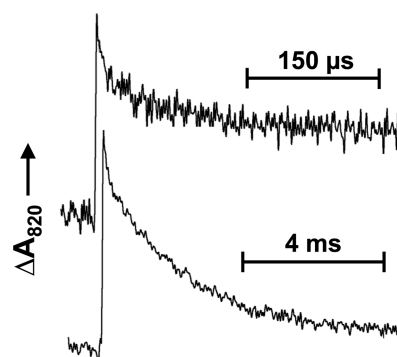


**Figure 1.** Kinetic traces showing PSI reduction by Cyt in the diatom *Phaeodactylum* on short (top) and longer (bottom) time scales. The bottom kinetic trace can be fit well to a biexponential curve, and the top trace corresponds to the first fast kinetic phase. The vertical arrow shows the direction of the absorbance increase. The standard reaction mixture contained, in a final volume of 0.2 mL, 20 mM Tricine-KOH (pH 7.5), 10 mM MgCl$_2$, 0.03% $\beta$-DM, an amount of PSI-enriched particles equivalent to 0.5 mg of Chl/mL, 0.1 mM methyl viologen, and 2 mM sodium ascorbate. The Cyt concentration was 150 $\mu$M. Other experimental conditions were as described in Experimental Procedures.
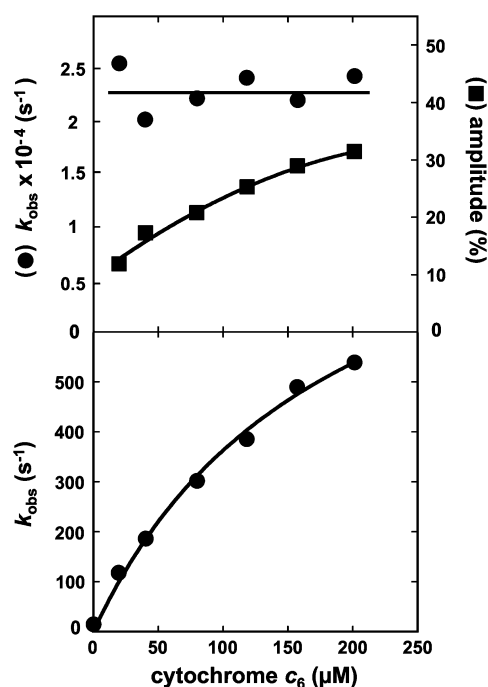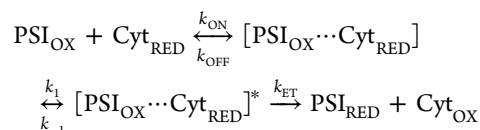


**Figure 2.** Dependence upon donor protein concentration (top) of the observed rate constant ($k_{obs}$) of the fast phase for *Phaeodactylum* PSI reduction by Cyt and of the amplitude of this phase with respect to the total absorbance change. Dependence of $k_{obs}$ for the slow phase (bottom) upon donor protein concentration. Other experimental conditions were as described in the legend of Figure 1.

$$\text{PSI}_{OX} + \text{Cyt}_{RED} \underset{k_{OFF}}{\overset{k_{ON}}{\rightleftharpoons}} [\text{PSI}_{OX}\cdots\text{Cyt}_{RED}]$$

$$\underset{k_{-1}}{\overset{k_1}{\rightleftharpoons}} [\text{PSI}_{OX}\cdots\text{Cyt}_{RED}]^* \overset{k_{ET}}{\longrightarrow} \text{PSI}_{RED} + \text{Cyt}_{OX}$$

where $k_{ON}$ and $k_{OFF}$ correspond to the association and dissociation rate constants for complex formation, respectively, from which the equilibrium association constant for this process ($K_A = k_{ON}/k_{OFF}$) is calculated; $k_1$ and $k_{-1}$ are the

**Table 1. Kinetic Parameters for PSI Reduction by Cyt in *Phaeodactylum* and the Cross Reactions with Other Prokaryotic and Eukaryotic Systems**

| PSI/donor couple | $k_{ON}{}^a$ (M$^{-1}$ s$^{-1}$) | $k_{OFF}{}^a$ (s$^{-1}$) | $K_A{}^a$ (M$^{-1}$) | $k_1{}^b$ (s$^{-1}$) | $k_{-1}{}^b$ (s$^{-1}$) | $K_R{}^b$ | $R_{MAX}{}^a$ (%) | $k_{ET}{}^b$ (s$^{-1}$) |
|---|---|---|---|---|---|---|---|---|
| *Phaeodactylum* PSI/*Phaeodactylum* Cyt | $5.9 \times 10^7$ | $9.8 \times 10^3$ | $6.0 \times 10^3$ | 1140 | 1700 | 0.67 | 37 | 21800 |
| *Phaeodactylum* PSI/*Monoraphidium* Cyt | $5.1 \times 10^7$ | $3.0 \times 10^3$ | $1.7 \times 10^4$ | 1480 | 3120 | 0.47 | 30 | 42900 |
| *Phaeodactylum* PSI/*Synechocystis* Cyt | $4.9 \times 10^7$ | $1.4 \times 10^4$ | $3.5 \times 10^3$ | – | – | – | – | 450 |
| *Nostoc* PSI/*Phaeodactylum* Cyt | $6.8 \times 10^7$ | $5.4 \times 10^3$ | $1.2 \times 10^4$ | – | – | – | – | 130 |
| *Arapidopsis* PSI/*Phaeodactylum* Cyt | $6.4 \times 10^7$ | $5.1 \times 10^3$ | $1.3 \times 10^4$ | – | – | – | – | 18700 |

$^a$Estimated according to the formalisms described by Meyer et al.[41] $^b$Estimated according to the formalism described by Sigfridsson et al.[34]

forward and the reverse rate constants, respectively, for complex rearrangement, from which is calculated the equilibrium constant ($K_R = k_1/k_{-1}$) for the rearrangement of the redox partners within the reaction complex to achieve the optimized ET configuration, marked as $[PSI_{ox}\cdots Cyt_{red}]^*$; and $k_{ET}$ is the subsequent ET first-order rate constant. By using the formalisms previously reported,[2,11,34] from the $k_{obs}$ of the fast phase, the amplitude of this phase extrapolated to infinite Cyt concentration [$R_{MAX}$, 37% (Table 1)], and the concentration dependence of the $k_{obs}$ values for the slower phase shown in Figure 2, it is possible to calculate minimal values for $k_{ON}$ and $k_{OFF}$ (and $K_A$) and for $k_1$ and $k_{-1}$ (and $K_R$), as well as the $k_{ET}$, all of which are listed in Table 1.

Considering the different electrostatic nature of the ET to PSI observed in other native systems from different types of organisms,[2,10,11,39,40,42,43] a comparative analysis of the effect of NaCl and MgCl$_2$ on the two phases of PSI reduction by Cyt was performed. Figure 3 (top) shows that an increasing NaCl concentration induces a drastic decrease in the percentage of the fast phase, which already exhibits a negligible amplitude at an ionic strength of 200 mM, although the $k_{obs}$ value for this phase (when detected) was not affected (not shown). However, the dependence of $k_{obs}$ for the slower phase on NaCl concentration showed a bell-shaped profile. This profile can be first explained as a salt-induced weakening of attractive electrostatic forces in the Cyt/PSI interaction at high NaCl concentrations, but also as a requirement for some flexibility of the redox partners inside the complex (to optimize ET) that is lacking at low ionic strengths, when overly strong electrostatic interactions freeze the complex in a nonoptimal configuration.[2,41]

A specific effect of Mg$^{2+}$ divalent cations has been previously described in some eukaryotic donor/PSI systems.[2,44−46] As shown in Figure 3 (bottom), a minimal concentration of Mg$^{2+}$ (2 mM, corresponding to an ionic strength of ∼30 mM) is required to allow the intracomplex Cyt/PSI reorganization leading to the fast kinetic phase, which shows a maximal amplitude at 10 mM MgCl$_2$ [corresponding to an ionic strength of ∼60 mM (Figure 3, bottom)]. This is indicative of a specific role of Mg$^{2+}$ cations, namely neutralization of repulsive interactions, by formation of a bridge between negative charges that hampers the complex reorganization. However, when the effect of salt on the slow kinetic phase was studied, the salt dependence of $k_{obs}$ exhibits a similar profile with both NaCl and MgCl$_2$ at equivalent ionic strengths (compare the top and bottom panels of Figure 3), thus suggesting that Mg$^{2+}$ does not play a specific role in the initial Cyt/PSI interaction and the formation of the encounter complex.

Taking into account that diatoms occupy a key branch in the evolutionary tree of oxygen-evolving photosynthetic organisms, but separate from the green lineage leading to higher plants,[13,15] we have performed cross reactions between Cyt donor proteins and PSI from selected cyanobacteria, green algae, and plant species (Figures 4 and 5). In the interaction of cyanobacterial (*Nostoc*) or plant (*Arabidopsis*) PSI with *Phaeodactylum* Cyt, no fast phase was observed (Figure 4, top), even though the protein concentration dependence of $k_{obs}$ exhibits in both cases saturation profiles (Figure 4, bottom), thus indicating transient complex formation prior to the ET step. This fact points to the subtle and specific set of interactions involved in the rearrangement process leading to the optimized configuration for ET in the native Cyt/PSI diatom couple, which are absent in these cross reaction systems. From the Cyt concentration dependence of $k_{obs}$, it is possible to calculate minimal values for both $K_A$ and $k_{ET}$,[41] which are listed in Table 1. Both preparations of PSI show $K_A$ values comparable to that calculated for the *Phaeodactylum* native system (Table 1), although a somewhat higher affinity ($K_A$ of ∼1.2 × 10$^4$ M$^{-1}$) toward *Phaeodactylum* Cyt was observed compared with that of the native system (Table 1). However,
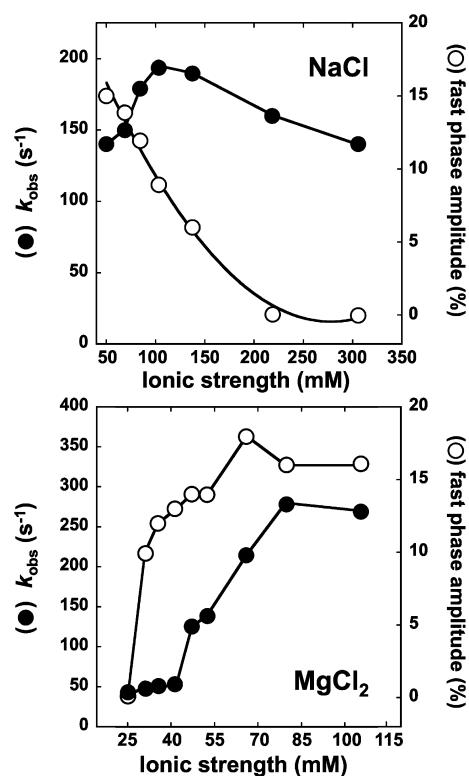


**Figure 3.** Plots of the observed rate constant ($k_{obs}$) of the slower phase and of the percentage of the fast phase for PSI reduction by Cyt vs ionic strength. The ionic strength was adjusted to the desired value by adding small amounts of concentrated NaCl (top) or MgCl$_2$ (bottom) stock solutions. The Cyt concentration was 60 μM. Other experimental conditions were as described in the legend of Figure 1.
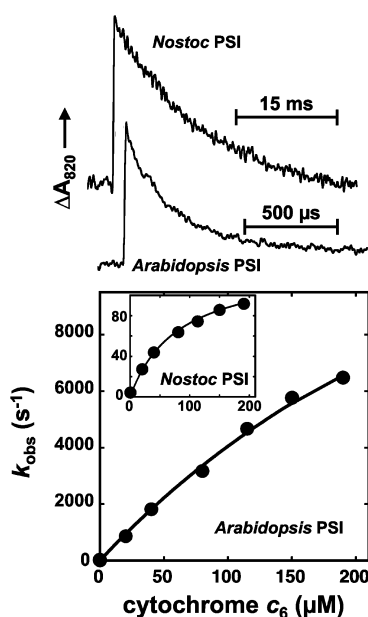
**Figure 4.** Cross reactions of *Phaeodactylum* Cyt with PSI from plant and cyanobacteria. Kinetic traces (top) showing *Nostoc* and *Arabidopsis* PSI reduction by *Phaeodactylum* Cyt. Both kinetic traces can be fit well to monoexponential curves. The concentration of Cyt was 100 $\mu$M. Dependence of $k_{obs}$ for *Arabidopsis* and *Nostoc* (inset) PSI reduction by *Phaeodactylum* Cyt (bottom) on donor protein concentration. Other experimental conditions were as described in the legend of Figure 1.
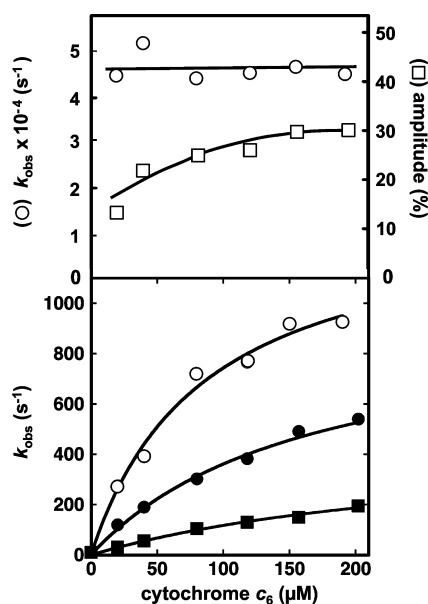


**Figure 5.** Cross reactions of *Phaeodactylum* PSI and Cyt from cyanobacteria and green alga. Dependence upon donor protein concentration of the $k_{obs}$ (top) of the fast phase for *Phaeodactylum* PSI reduction by *Monoraphidium* Cyt and of the amplitude of this phase with respect to the total absorbance change. Dependence of $k_{obs}$ for *Phaeodactylum* PSI reduction by *Phaeodactylum* [slower phase (●)], *Monoraphidium* [slower phase (○)], and *Synechocystis* (■) Cyt (bottom) on donor protein concentration. Other experimental conditions were as described in the legend of Figure 1.

whereas the cyanobacterial PSI exhibited a very low $k_{ET}$, indicating the formation of a nonoptimized ET complex with the diatom Cyt, the plant photosystem presented an estimated $k_{ET}$ value (18700 s$^{-1}$) on the same order of magnitude as that

exhibited by the *Phaeodactylum* native system (Table 1). With regard to the electrostatic nature of the Cyt/PSI interaction, cyanobacterial and plant PSIs behave in an opposite way when the NaCl concentration is increased (not shown). Thus, *Phaeodactylum* Cyt interacts with plant PSI by means of strong attractive forces, as inferred from the drastic and continuous decrease in $k_{obs}$ with an increasing ionic strength (not shown). However, *Nostoc* PSI shows moderate repulsive electrostatic interactions with the diatom Cyt, as deduced from the also continuous, although much less pronounced, increase in $k_{obs}$ with an increase in ionic strength (not shown).

Upon analysis of the reduction of *Phaeodactylum* PSI by cyanobacterial (*Synechocystis*) Cyt, no fast phase was observed, although the nonlinear donor protein concentration dependence of $k_{obs}$ (Figure 5, bottom) also indicates the transient formation of a bimolecular complex (the estimated minimal values for $K_A$ and $k_{ET}$ are listed in Table 1). Figure 5 also includes the concentration dependence of the slower phase of the native *Phaeodactylum* system, for comparative purposes. The cyanobacterial *Synechocystis* Cyt shows low values for both association and ET constants with the diatom PSI, indicating again the formation of a nonoptimized ET complex. However, upon analysis of the interaction of green alga (*Monoraphidium*) Cyt with diatom PSI, kinetic traces have to be fit to biphasic curves (not shown), as was the case for the native diatom system, with the fast phase reaching saturating values of 30% (Figure 5, top). The concentration-independent $k_{obs}$ for such a fast phase has an average value of 46000 s$^{-1}$ ($t_{1/2}$ of ~15 $\mu$s) (Figure 5, top), thus indicating an efficient first-order ET process occurring in the preformed [Cyt/PSI] transient complex. This ET rate constant value is twice that of the diatom native system and is close to the values of plant and green alga systems.[1,2,34,40]

As in the case of the native diatom system, the *Monoraphidium* Cyt concentration dependence of $k_{obs}$ for the slower phase of PSI reduction shows a saturation profile (Figure 5, bottom). Again, the theoretical $k_{obs}$ value (1380 s$^{-1}$) obtained by extrapolating to an infinite donor protein concentration[41] does not match the experimental $k_{obs}$ data for the fast phase, thus suggesting the occurrence of a rearrangement step prior to ET. The minimal values for $K_A$ and $K_R$, as well as the $k_{ET}$, are listed in Table 1. Via comparison of the $K_A$ values, the *Monoraphidium* Cyt has a higher affinity for *Phaeodactylum* PSI than the native diatom Cyt, whereas the $K_R$ value is lower than that obtained for the native couple.

As previously shown for the cyanobacterial PSI/diatom Cyt cross reaction, *Phaeodactylum* PSI shows repulsive electrostatic interactions with *Synechocystis* Cyt, as deduced from the increase in $k_{obs}$ with an increasing NaCl concentration (not shown). The $k_{obs}$ for the slow phase of diatom PSI reduction by *Monoraphidium* Cyt showed, however, a bell-shaped profile with an increase in ionic strength (not shown), indicating the existence of some reorientation of redox partners inside the transient complex prior to the ET step, as already deduced from the biphasic kinetic traces.

## ■ DISCUSSION

The interaction of Cyt (and the functionally equivalent Pc) with PSI has been studied by fast kinetic analysis in a wide variety of evolutionarily differentiated organisms, mainly belonging to the green lineage that evolved to higher plants.[1,2,10,34,39,40,42,43,47−49] This large set of data has allowed the proposal of different reaction mechanisms for the ET to PSI
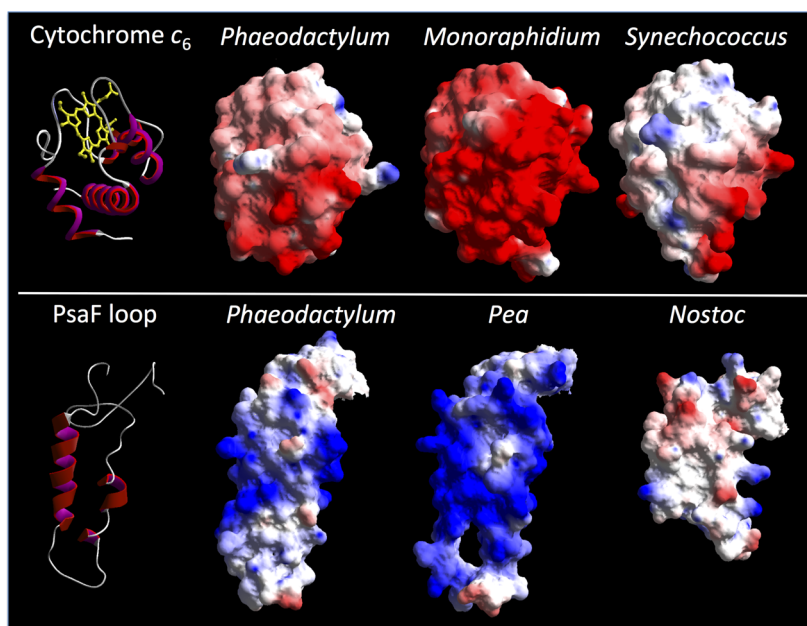
**Figure 6.** Surface electrostatic potential distribution of (top) Cyt from *Phaeodactylum*, *Monoraphidium*, and *Thermosynechococcus* and (bottom) the PsaF luminal loop from *Phaeodactylum*, pea, and *Nostoc*. The view of the cytochromes shows in front the loop containing the sixth axial ligand and the heme propionates pointing upward. This view also presents in front the protein surface proposed to be responsible for electrostatic interactions with PSI. The PsaF loops of *Phaeodactylum* and *Nostoc* were modeled using Phyre[2]. The PsaF of *Nostoc* lacks the loop exclusive of eukaryotic PsaFs. Simulations of the surface electrostatic potential distribution were performed assuming an ionic strength of 100 mM at pH 7.0. Positively and negatively charged regions are colored blue and red, respectively.

and also models for how this mechanism has evolved (reviewed in refs 1 and 50). Pc and Cyt from eukaryotic organisms, in particular, mostly appear to react with PSI by following a three-step reaction mechanism (type III), which involves formation of an electrostatically driven transient complex, further rearrangement of redox partners inside the complex, and, finally, ET. In some cyanobacteria, however, it is also possible to observe a simple oriented collisional mechanism, with no formation of any detectable transient complex (type I), whereas in other cyanobacteria and in ferns, a two-step mechanism involving transient complex formation prior to ET but no complex rearrangement (type II) is observed.

Diatoms arose from double endosymbiosis events that confer to these organisms singular metabolic pathways, including a central role of the mitochondria in the management of energy and the metabolism of carbon and nitrogen, as well as the existence of a complete urea cycle.[12−15] In addition, diatom chloroplasts are engulfed by four membranes. These specific features, as well as the presence of the siliceous external envelope, can explain the relatively low content of photosynthetic complexes in diatoms compared to that of cyanobacteria, green algae, or plant cells. Although there are also differences in the thylakoid organization in stacked regions and the distribution of photosystems,[13,15] the structural bases of the photosynthetic electron transfer flow are basically the same in the green and red lineages, including the role played by Cyt (and/or Pc) in connecting the $b_6f$ and PSI complexes.

The reduction of *Phaeodactylum* PSI by Cyt can be explained as following a type III mechanism, as indicated by the occurrence of biphasic kinetics and the Cyt concentration dependence of the $k_{obs}$ for both phases. However, it has to be noted that although the type III model, based on the reconfiguration of the PSI/donor complex prior to ET, has usually been adopted, an alternative hypothesis was recently

proposed (discussed in ref 51), associated with a low reorganization energy for the ET step (~0.6 eV) rather than with a rate-limiting rearrangement of the ET complex.[51,52] Thus, the analysis of the *in vivo* reduction of $P_{700}^+$ by Pc in the green alga *Chlamydomonas reinhardtii* was proposed to be consistent with the formation of a relatively tight binary complex, which does not undergo kinetically limiting conformational reconfiguration, the activation barrier for the ET step being determined mainly by enthalpic contributions to the free energy change.[51] According to this proposal, strong electrostatic interactions in the eukaryotic systems might serve not only to ensure tight binding and a high affinity but also to exclude water molecules from the binding site during complex formation. This exclusion would minimize water reorganization in the ET step, reducing in this way the entropic contribution, and thus the total reorganization energy of the process.[51] Although such a hypothesis could be reasonably extended to the system investigated in our study, which exhibits characteristics intermediate between those of the green lineage and the cyanobacterial systems, in the case of ET from Cyt (instead of Pc) to PSI, the effect of solvent reorganization of the redox active iron atom is mitigated by coupling with the extended π-system of the porphyrin ring.[51] In addition, the bell-shaped profile of the dependence of rate constant on salt concentration shown in Figure 3 indicates the requirement of certain flexibility of the redox partners inside the complex and, consequently, supports some intracomplex rearrangement, consistent with a type III mechanism. Both the first-order $k_{ET}$ (21800 vs ~70000−80000) and the maximal percentage values of amplitude (37% vs ~50−75%) for the preformed [Cyt/PSI] complex are lower than the reported values for green alga and plant systems.[2,34,40,43] Consequently, the $K_R$ value (0.65) is also lower in *Phaeodactylum* than in other "green" eukaryotic systems (ranging from 4 to 7).[2,34,40] These findings indicate

that the "red" *Phaeodactylum* system possesses a lower efficiency than the "green" systems, both in the formation of the properly arranged [Cyt/PSI] complex and in the ET itself.

The $K_A$ value reported here for the Cyt/PSI system from *Phaeodactylum* ($6 \times 10^3$ M$^{-1}$) is also lower than those reported for donor/PSI couples from green algae and higher plants (typically ranging from $10^4$ to $10^5$ M$^{-1}$).[2,34,40,49] This can be explained in terms of the intensity of the electrostatic interactions between the soluble donor and PSI. Thus, although the ionic strength dependence data make clear the occurrence of attractive electrostatic interactions between *Phaeodactylum* Cyt and PSI, the magnitude of such an interaction is quite low, as indicated by the smooth decrease in $k_{obs}$ at high ionic strengths shown in Figure 3. This behavior drastically contrasts with the strong dependence observed in other eukaryotic green systems,[2,39,45,49] suggesting the existence of significant electrostatic differences between the heme protein and/or PSI in the green and red lineages. In these sense, it is well established that in green algae and higher plants, a positively charged luminal extended loop in the PsaF subunit of the PSI complex, absent in cyanobacteria, is responsible for both the electrostatic interaction between PSI and the negatively charged donor and the correct positioning of both partners for an optimal ET (Figure 6); this last step involves long-range electrostatic attractions between basic patches of PsaF and acidic regions of both Pc and Cyt, as well as hydrophobic interactions.[7,8,53,54] However, as shown in Figure 6, although it preserves the extra loop, the positive character of the PsaF luminal region is significantly diminished in *Phaeodactylum*, as a result of the absence of basic residues, indeed present in green algae and higher plants, and the presence of additional negative residues (Figure S2 of the Supporting Information). In addition, although the determined crystal structure of *Phaeodactylum* Cyt[21] shows that the diatom protein maintains the overall structure previously described for other Cyts,[55−57] the decrease in the number of positive charges in the diatom PsaF is accompanied by a similar decrease in the negative acidic area on Cyt (Figure 6 and Figure S2 of the Supporting Information), demonstrated to be involved in the interaction with PSI in other organisms (reviewed in ref 50). Thus, the occurrence of diminished basic patches on PsaF and acidic regions on Cyt promotes a weaker electrostatic interaction between partners, a decrease in protein/protein affinity, and a lower efficiency for the formation of the optimized ET complex, as compared with those of the green lineage systems. In previous studies of donor/PSI systems from green algae and plants, it has been suggested that the donor exchange from PSI represents the kinetic limiting step in the ET between cytochrome $b_6f$ and PSI complexes.[8,43] Thus, a weaker electrostatic interaction and a decreased affinity for Cyt in diatoms can represent a compromise between ET efficiency and the donor release required for an optimal linear ET between the two photosynthetic membrane complexes.

The different structural and electrostatic features of PSI and Cyt from different sources also explain the results obtained in the cross reactions analyzed here. It is interesting to note that cross reactions involving the green and red lineages (e.g., diatom Cyt/plant PSI and green alga Cyt/diatom PSI) show kinetic parameters comparable to, or even better than, those of the native diatom system, although they follow different kinetic mechanisms. In the case of green alga Cyt reacting with diatom PSI, both higher $K_A$ and $k_{et}$ values were observed as compared with those of the *Phaeodactylum* native system, whereas plant

PSI shows a $k_{et}$ value with the diatom Cyt comparable to that of the diatom native couple. Thus, a stronger electrostatic charge in just one of the partners is enough to support, in both cases, an efficient ET rate. In fact, and in agreement with the occurrence of stronger electrostatic complementary interactions, both eukaryotic Cyt/PSI cross reactions show a marked decrease in efficiency as ionic strength increases, as compared with the weak effect observed in the native diatom system (not shown). However, in both cases, this stronger electrostatic interaction affects the fine adjustment involved in the complex rearrangement leading to the optimal functional configuration. First, the diatom Cyt/plant PSI system proceeds via a type II mechanism, with the absence of the final rearrangement step, although *Phaeodactylum* Cyt is able to bind with high affinity and to form an efficient encounter complex with plant PSI, as shown by the high $k_{ET}$ value (18700 s$^{-1}$), comparable to that of the native system. Second, although the reduction of diatom PSI by the strongly acidic Cyt from the green alga follows a type III mechanism, showing a $k_{ET}$ value twice that of the native diatom system and closer to those of other eukaryotic systems, the maximal percentage of the fast phase and the $K_R$ are smaller than in the diatom native system (Table 1). These findings indicate that the latter cross reaction possesses a relatively lower efficiency of formation of the properly arranged [Cyt/PSI] complex. Moreover, these data suggest that it is mainly the different electrostatic properties of Cyt, more than those of the PSI, that make the difference in the behavior of the diatom system with respect to that of other eukaryotic systems.

Unlike eukaryotic photosynthetic organisms, PsaF does not appear to play a significant role in the donor/PSI interaction in cyanobacteria,[53] as this PSI subunit does not possess either the extra luminal loop or a strong positive character (Figure 6).[58] As a consequence of the absence of this basic patch on PSI, the complex formed by *Phaeodactylum* Cyt and cyanobacterial PSI shows the lower ET efficiency of the systems here analyzed, reflecting a nonoptimal configuration of the ET complex, which also occurs when the slightly acidic *Synechocystis* Cyt interacts with the diatom PSI. All these data reveal the specific set of interactions involved in the recognition and efficient ET in the diatom Cyt/PSI native system.

As a final conclusion, the kinetic analysis reported here for PSI reduction by Cyt in the diatom *Phaeodactylum* reinforces previous observations that evolution, from the ancient neutral or positively charged soluble donors in cyanobacteria to the negatively charged donors in eukaryotes, involved parallel and complementary structural and dynamic changes, not only in the donor proteins but also in PSI. Although the evolution of the ET to PSI in *Phaeodactylum* has led to complementary electrostatic interactions between acidic and basic patches in Cyt and PsaF, respectively, the electrostatic character of both partners is similarly reduced, as is the intensity of the interaction as compared with the strongest electrostatic properties of the Cyt(Pc)/PSI complex in the green lineage leading to higher plants.

## ■ ASSOCIATED CONTENT

### ⑤ Supporting Information

Equations used in the fitting of the experimental data to the kinetic model derived from the proposed reaction mechanism (Figure S1) and protein sequence alignments of *Phaeodactylum* Cyt and PsaF with other equivalent proteins from cyanobacteria, green algae, and plants (Figure S2). This material is available free of charge via the Internet at http://pubs.acs.org.

## AUTHOR INFORMATION

### Corresponding Author
*Instituto de Bioquímica Vegetal y Fotosíntesis, Centro de Investigaciones Científicas Isla de la Cartuja, Universidad de Sevilla & CSIC, Américo Vespucio 49, 41092 Sevilla, Spain. Telephone: 34-954-489-515. Fax: 34-954-460-165. E-mail: jnavarro@ibvf.csic.es.

### Notes
The authors declare no competing financial interest.

## ACKNOWLEDGMENTS

## ABBREVIATIONS

$\beta$-DM, $\beta$-dodecyl maltoside; Cyt, cytochrome $c_6$; ET, electron transfer; FCP, chlorophyll $c$/fucoxanthin-containing light-harvesting complexes; $k_2$, second-order rate constant; $K_A$, equilibrium constant for the complex formation reaction; $k_{et}$, first-order electron transfer rate constant; $k_{obs}$, observed pseudo-first-order rate constant; $k_{ON}$ and $k_{OFF}$, association and dissociation rate constants, respectively, for complex formation; $k_1$ and $k_{-1}$, forward and reverse rate constants, respectively, for complex rearrangement; $K_R$, equilibrium constant for rearrangement of redox proteins within the reaction complex; Pc, plastocyanin; PSI, photosystem I; $R_{MAX}$, amplitude of the fast phase for photosystem I reduction extrapolated to an infinite donor concentration.

## REFERENCES

(1) Hervás, M., Navarro, J. A., and De la Rosa, M. A. (2003) Electron transfer between soluble proteins and membrane complexes in photosynthesis. *Acc. Chem. Res. 36*, 798−805.

(2) Hervás, M., Navarro, J. A., Díaz, A., Bottin, H., and De la Rosa, M. A. (1995) Laser-flash kinetic analysis of the fast electron transfer from plastocyanin and cytochrome $c_6$ to photosystem I. Experimental evidence on the evolution of the reaction mechanism. *Biochemistry 34*, 11321−11326.

(3) Hope, A. B. (2000) Electron transfer amongst cytochrome *f*, plastocyanin and photosystem I: Kinetics and mechanisms. *Biochim. Biophys. Acta 1456*, 5−26.

(4) De la Rosa, M. A., Navarro, J. A., Díaz-Quintana, A., De la Cerda, B., Molina-Heredia, F. P., Balme, A., Murdoch, P. S., Díaz-Moreno, I., Durán, R. V., and Hervás, M. (2002) An evolutionary analysis of the reaction mechanisms of photosystem I reduction by cytochrome $c_6$ and plastocyanin. *Bioelectrochemistry 55*, 41−45.

(5) Durán, R. V., Hervás, M., De la Rosa, M. A., and Navarro, J. A. (2005) *In vivo* photosystem I reduction in thermophilic and mesophilic cyanobacteria: The thermal resistance of the process is limited by factors other than the unfolding of the partners. *Biochem. Biophys. Res. Commun. 334*, 170−175.

(6) Ben-Shem, A., Frolow, F., and Nelson, N. (2003) Crystal structure of plant photosystem I. *Nature 426*, 630−635.

(7) Fromme, P., Melkozernov, A., Jordan, P., and Krauss, N. (2003) Structure and function of photosystem I: Interaction with its soluble electron carriers and external antenna systems. *FEBS Lett. 555*, 40−44.

(8) Busch, A., and Hippler, M. (2011) The structure and function of eukaryotic photosystem I. *Biochim. Biophys. Acta 1807*, 864−877.

(9) Hervás, M., Navarro, J. A., Díaz, A., and De la Rosa, M. A. (1996) A comparative thermodynamic analysis by laser-flash absorption spectroscopy of photosystem I reduction by plastocyanin and cytochrome $c_6$ in *Anabaena* PCC 7119, *Synechocystis* PCC 6803, and spinach. *Biochemistry 35*, 2693−2698.

(10) Molina-Heredia, F. P., Hervás, M., Navarro, J. A., and De la Rosa, M. A. (2001) A single arginyl residue in plastocyanin and cytochrome $c_6$ from the cyanobacterium *Anabaena sp.* PCC 7119 is required for efficient reduction of photosystem I. *J. Biol. Chem. 276*, 601−605.

(11) Hervás, M., Díaz-Quintana, A., Kerfeld, C., Krogmann, D., De la Rosa, M. A., and Navarro, J. A. (2005) Cyanobacterial Photosystem I lacks specificity in its interaction with cytochrome $c_6$ electron donors. *Photosynth. Res. 83*, 329−333.

(12) Bowler, C., Allen, A. E., Badger, J. H., et al. (2008) The *Phaeodactylum* genome reveals the evolutionary history of diatom genomes. *Nature 456*, 239−244.

(13) Grouneva, I., Gollan, P. J., Kangasjärvi, S., Suorsa, M., Tikkanen, M., and Aro, E.-M. (2013) Phylogenetic viewpoints on regulation of light harvesting and electron transport in eukaryotic photosynthetic organisms. *Planta 237*, 399−412.

(14) Kooistra, W. H. C. F., Gersonde, R., Medlin, L. K., and Mann, D. G. (2007) The origin and evolution of the diatoms: Their adaptation to a planktonic existence. In *Evolution of Primary Producers in the Sea* (Falkowski, P. G., and Knoll, A. H., Eds.) pp 207−249, Academic Press, Inc., New York.

(15) Bowler, C., Vardi, A., and Allen, A. E. (2010) Oceanographic and biogeochemical insights from diatom genomes. *Annual Reviews of Marine Science 2*, 333−365.

(16) Nelson, D. M., Tréguer, P., Brzezinski, M. A., Leynaert, A., and Quéguiner, B. (1995) Production and dissolution of biogenic silica in the ocean: Revised global estimates, comparison with regional data and relationship to biogenic sedimentation. *Global Biogeochem. Cycles 9*, 359−372.

(17) Falkowski, P. G., Fenchel, T., and Delong, E. F. (2008) The microbial engines that drive Earth's biogeochemical cycles. *Science 320*, 1034−1039.

(18) Nagao, R., Moriguchi, A., Tomo, T., Niikura, A., Nakajima, S., Suzuki, T., Okumura, A., Iwai, M., Shen, R.-S., Ikeuchi, M., and Enami, I. (2010) Binding and functional properties of five extrinsic proteins in oxygen-evolving photosystem II from a marine centric diatom, *Chaetoceros gracilis. J. Biol. Chem. 285*, 29191−29199.

(19) Nagao, R., Ishii, A., Tada, O., Suzuki, T., Dohmae, N., Okumura, A., Iwai, M., Takahashi, T., Kashino, Y., and Enami, I. (2007) Isolation and characterization of oxygen-evolving thylakoid membranes and Photosystem II particles from a marine diatom *Chaetoceros gracilis. Biochim. Biophys. Acta 1767*, 1353−1362.

(20) Veith, T., and Büchel, C. (2007) The monomeric photosystem I-complex of the diatom *Phaeodactylum tricornutum* binds specific fucoxanthin chlorophyll proteins (FCPs) as light-harvesting complexes. *Biochim. Biophys. Acta 1767*, 1428−1435.

(21) Akazaki, H., Kawai, F., Hosokawa, M., Hama, T., Chida, H., Hirano, T., Lim, B.-K., Sakurai, N., Hakamata, W., Park, S.-Y., Nishio, T., and Oku, T. (2009) Crystallization and structural analysis of cytochrome $c_6$ from the diatom *Phaeodactylum tricornutum* at 1.5 Å resolution. *Biosci., Biotechnol., Biochem. 73*, 189−191.

(22) Peers, G., and Price, N. M. (2006) Copper-containing plastocyanin used for electron transport by an oceanic diatom. *Nature 441*, 341−344.

(23) Shimazaki, K., Takamiya, K., and Nishimura, M. (1978) Studies on electron transfer systems in the marine diatom *Phaeodactylum tricornutum. J. Biochem. 83*, 1631−1638.

(24) Berkaloff, C., Caron, L., and Rousseau, B. (1990) Subunit organization of PSI particles from brown algae and diatoms: Polypeptide and pigment analysis. *Photosynth. Res. 23*, 181−193.

(25) Lepetit, B., Volke, D., Szabó, M., Hoffmann, R., Garab, G., Wilhelm, C., and Goss, R. (2007) Spectroscopic and molecular characterization of the oligomeric antenna of the diatom *Phaeodactylum tricornutum. Biochemistry 46*, 9813−9822.

(26) Ikeda, Y., Kashino, Y., Koike, H., and Satoh, K. (2008) Purification and the antenna size of photosystem I complexes from a centric diatom, *Chaetoceros gracilis*. In *Photosynthesis. Energy from the Sun: 14th International Congress on Photosynthesis* (Allen, J. F., Gantt, E., Golbeck, J. H., and Osmond, B., Eds.) pp 269−272, Springer, Berlin.

(27) Lepetit, B., Volke, D., Gilbert, M., Wilhelm, C., and Goss, R. (2010) Evidence for the existence of one antenna-associated, lipid-dissolved and two protein bound pools of diadinoxanthin cycle pigments in diatoms. *Plant Physiol. 154*, 1905−1920.

(28) Juhas, M., and Büchel, C. (2102) Properties of photosystem I antenna protein complexes of the diatom *Cyclotella meneghiniana*. *J. Exp. Bot. 63*, 3673−3682.

(29) Gundermann, K., Schmidt, M., Weisheit, W., Mittag, M., and Büchel, C. (2013) Identification of several sub-populations in the pool of light harvesting proteins in the pennate diatom *Phaeodactylum tricornutum*. *Biochim. Biophys. Acta 1827*, 303−310.

(30) Navarro, J. A., Hervás, M., and De la Rosa, M. A. (2011) Purification of plastocyanin and cytochrome $c_6$ from plants, green algae, and cyanobacteria. In *Photosynthesis Protocols* (Carpentier, R., Ed.) Vol. *684*, pp 79−94, Humana Press, Totowa, NJ.

(31) Mathis, P., and Sétif, P. (1981) Near infra-red absorption spectra of the chlorophyll *a* cations and triplet state *in vitro* and *in vivo*. *Isr. J. Chem. 21*, 316−320.

(32) Arnon, D. I. (1949) Copper enzymes in isolated chloroplasts. *Plant Physiol. 24*, 1−15.

(33) Hervás, M., and Navarro, J. A. (2011) Effect of crowding on the electron transfer process from plastocyanin and cytochrome $c_6$ to photosystem-I: A comparative study from cyanobacteria to green algae. *Photosynth. Res. 107*, 279−286.

(34) Sigfridsson, K., He, S., Modi, S., Bendall, D. S., Gray, J., and Hansson, Ö. (1996) A comparative flash-photolysis study of electron transfer from pea and spinach plastocyanins to spinach photosystem I. A reaction involving a rate-limiting conformational change. *Photosynth. Res. 50*, 11−21.

(35) Kelley, L. A., and Sternberg, M. J. E. (2009) Protein structure prediction on the web: A case study using the Phyre server. *Nat. Protoc. 4*, 363−371.

(36) Laskowski, R. A., McArthur, M. W., Moss, D. S., and Thornton, J. M. (1993) PROCHECK: A program to check the stereochemical quality of protein structures. *J. Appl. Crystallogr. 26*, 283−291.

(37) Guex, N., and Peitsch, M. C. (1997) SWISS-MODEL and the Swiss-PdbViewer: An environment for comparative protein modelling. *Electrophoresis 18*, 2714−2723.

(38) Sigfridsson, K., Young, S., and Hansson, Ö. (1996) Structural dynamics in the plastocyanin-photosystem I electron-transfer complex as revealed by mutant studies. *Biochemistry 35*, 1249−1257.

(39) Sigfridsson, K., Young, S., and Hansson, Ö. (1997) Electron transfer between spinach plastocyanin mutants and photosystem 1. *Eur. J. Biochem. 245*, 801−812.

(40) Sommer, F., Drepper, F., and Hippler, M. (2002) The luminal helix l of PsaB is essential for recognition of plastocyanin or cytochrome $c_6$ and fast electron transfer to photosystem I in *Chlamydomonas reinhardtii*. *J. Biol. Chem. 277*, 6573−6581.

(41) Meyer, T. E., Zhao, Z. G., Cusanovich, M. A., and Tollin, G. (1993) Transient kinetics of electron transfer from a variety of c-type cytochromes to plastocyanin. *Biochemistry 32*, 4552−4559.

(42) Molina-Heredia, F. P., Wastl, J., Navarro, J. A., Bendall, D., Hervás, M., Howe, C., and De la Rosa, M. A. (2003) A new function for an old cytochrome? *Nature 424*, 33−34.

(43) Drepper, F., Hippler, M., Nitschke, W., and Haehnel, W. (1996) Binding dynamics and electron transfer between plastocyanin and photosystem I. *Biochemistry 35*, 1282−1295.

(44) Haehnel, W., Pröpper, A., and Krause, H. (1980) Evidence for complexed plastocyanin as the immediate electron donor of P-700. *Biochim. Biophys. Acta 593*, 384−399.

(45) Hervás, M., De la Rosa, M. A., and Tollin, G. (1992) A comparative laser flash photolysis study of algal plastocyanin and cytochrome c552 photooxidation by photosystem I particles from spinach. *Eur. J. Biochem. 203*, 115−120.

(46) Medina, M., Díaz, A., Hervás, M., Navarro, J. A., Gómez-Moreno, C., De la Rosa, M. A., and Tollin, G. (1993) A comparative laser flash absorption spectroscopy study of *Anabaena* PCC 7119 plastocyanin and cytochrome $c_6$ photooxidation by photosystem I particles. *Eur. J. Biochem. 213*, 1133−1138.

(47) Bottin, H., and Mathis, P. (1985) Interaction of plastocyanin with the photosystem I reaction center: A kinetic study by flash absorption spectroscopy. *Biochemistry 24*, 6453−6460.

(48) Hervás, M., Ortega, J. M., Navarro, J. A., De la Rosa, M. A., and Bottin, H. (1994) Laser flash kinetic analysis of *Synechocystis* PCC 6803 cytochrome $c_6$ and plastocyanin oxidation by photosystem I. *Biochim. Biophys. Acta 1184*, 235−241.

(49) Sommer, F., Drepper, F., Haehnel, W., and Hippler, M. (2004) The hydrophobic recognition site formed by residues PsaA-Trp651 and PsaB-Trp627 of photosystem I in *Chlamydomonas reinhardtii* confers distinct selectivity for binding of plastocyanin and cytochrome $c_6$. *J. Biol. Chem. 279*, 20009−20017.

(50) Díaz-Quintana, A., Hervás, M., Navarro, J. A., and De la Rosa, M. A. (2008) Plastocyanin and cytochrome $c_6$: The soluble electron carriers between the cytochrome $b_6f$ complex and photosystem I. In *Photosynthetic Protein Complexes: A Structural Approach* (Fromme, P., Ed.) pp 181−200, Wiley-VCH Verlag Gmbh & Co. KGaA, Weinheim, Germany.

(51) Santabarbara, S., Redding, K. E., and Rappaport, F. (2009) Temperature dependence of the reduction of $P_{700}^+$ by tightly bound plastocyanin in vivo. *Biochemistry 48*, 10457−10466.

(52) Ramesh, V. M., Guergova-Kuras, M., Joliot, P., and Webber, A. N. (2002) Electron transfer from plastocyanin to the photosystem I reaction center in mutants with increased potential of the primary donor in *Chlamydomonas reinhardtii*. *Biochemistry 41*, 14652−14658.

(53) Hippler, M., Reichert, J., Sutter, M., Zak, E., Altschmied, L., Schröer, U., Herrmann, R. G., and Haehnel, W. (1996) The plastocyanin binding domain of photosystem I. *EMBO J. 15*, 6374−6384.

(54) Hippler, M., Drepper, F., Rochaix, J. D., and Mühlenhoff, U. (1999) Insertion of the N-terminal part of PsaF from *Chlamydomonas reinhardtii* into photosystem I from *Synechococcus elongatus* enables efficient binding of algal plastocyanin and cytochrome $c_6$. *J. Biol. Chem. 274*, 4180−4188.

(55) Frazão, C., Soares, C. M., Carrondo, M. A., Pohl, E., Dauter, Z., Wilson, K. S., Hervás, M., Navarro, J. A., De la Rosa, M. A., and Sheldrick, G. (1995) *Ab initio* determination of the crystal structure of cytochrome $c_6$ and comparison with plastocyanin. *Structure 3*, 1159−1169.

(56) Kerfeld, C. A., Anwar, H. P., Interrante, R., Merchant, S., and Yeates, T. O. (1995) The structure of chloroplast cytochrome $c_6$ at 1.9 Å resolution: Evidence for functional oligomerization. *J. Mol. Biol. 250*, 627−647.

(57) Yamada, S., Park, S. Y., Shimizu, H., Koshizuka, Y., Kadokura, K., Satoh, T., Suruga, K., Ogawa, M., Isogai, Y., Nishio, T., Shiro, Y., and Oku, T. (2000) Structure of cytochrome $c_6$ from the red alga *Porphyra yezoensis* at 1.57 Å resolution. *Acta Crystallogr. D56*, 1577−1582.

(58) Fromme, P., Jordan, P., and Krauss, N. (2001) Structure of photosystem I. *Biochim. Biophys. Acta 1507*, 5−31.